JUMP PHENOMENA IN FREQUENCY RESPONSE SPECTRA DUE TO THE USE OF MECHANICAL EXCITER

Priyosulistyo *)

ABSTRACT

Jump phenomena commonly occurred on vibration tests of structures with soft or hard spring systems. These phenomena normally caused lost of data at about resonant frequencies. The steady state vibration test, using a mechanical exciter as well as a magnetic exciter, on a simple reinforced concrete beam with linear spring system, has also shown such jump phenomena.

To investigate the phenomena, a differential equation of two degrees of freedom system was set up representing the mass of the structure and the moving mass of the exciter. Two sets of steady state vibration test using the mechanical and magnetic exciters were carried out. Accordingly, results of the test were graphically compared to the theory developed.

The investigation shows that such phenomena are due to the effect of phase difference of the two masses (excited mass and the moving mass of exciter) when approaching resonance. These phase differences trigger the force of excitation away from the direction of the induced force / reflected force. As the results, the applied force is reduced and becomes unstable. The unstable force is furtherly indicated as the jump phenomena. The larger the force of the excitation and the lower the damping ratio of the excited structure, the wider the unstable region where the jump phenomena as well as the sudden drop are possible to occur. Both theoretical and experimental graphs of the linear simple reinforced beam indicate similarities to the structures with non-linear hard spring system.

INTRODUCTION

White ,1971 and 1973, developed a theory of structures with non-linear soft spring and hard spring systems. He introduced a boundary equation where unstable region could occur.

Tomlinson et al., 1979 and 1980, investigated a structure using Coulomb friction damping in polar plots. The friction damping changed the shape of the polar plots. The friction, working at lower amplitudes of excitation, dragged the polar plots away from the center of the axes created "pear alike".

Rades, 1983, furtherly applied the theory suggested by White (1971), using a beam with pin-supports at the ends. Under high amplitude of excitation, the beam indicated a jump phenomenon. The membrane effect has been claimed as the cause of the phenomenon where stiffness of the beam behaved non-linearly hard spring. The previous experiment (Rades, 1982 and 1983) using both combined Coulomb and hysteretic damping and quadratic damping did not indicate any jump phenomenon. The distorted polar plots were claimed as the result of the use of the quadratic damping.

A reinforced concrete beam upon simple supports (hinge and roller) was tested under vibrations. The beam was supposed to respond as a linear spring system, but in fact, Priyosulistyo (1988) reported that the response of the steady state test using a mechanical exciter was jagged about the resonance and was indicating a jump phenomenon. The jump phenomenon made hesitation in predicting resonant frequency as well as its amplitude. The last two parameters are of important in the detection of cracks of structures under investigation. Further study of this phenomenon was investigated by setting up two exciters, i.e. the mechanical exciter and the magnetic exciter, mounted on the same reinforced concrete beam at about the same position and by exciting the beams over its resonant frequency.

The out of balance mass of the mechanical exciter produces force proportional to its squared frequency. Therefore, increasing the frequency of excitation by a frequency controller results in higher force of excitation. A linear change of force of excitation, if required, can be carried out by adjusting the out of balance mass which comprise two sets of solid half circle steel attached at both ends of the exciter shaft. Two different series of force of excitation were applied on the beam over the first mode. Forward and reverse frequency excitations were carried out to examine the behaviour of the jump phenomenon.

MATHEMATICAL MODEL

Absolute and Relative Parameters.

Assuming that the exciter has constant and high magnetic fields the problem is now to determine the

*) staff members of Inter University Center for Engineering Science, Gadjah Mada University

relative phases and amplitudes of the moving exciter mass to the beam. The relationships may be explainable in fig.1. The relative displacement of the moving exciter mass to the beam is assumed as :

$$x_1 = A \sin \omega t \qquad (1)$$

where :A = invisible relative amplitude coefficient of the moving exciter mass.

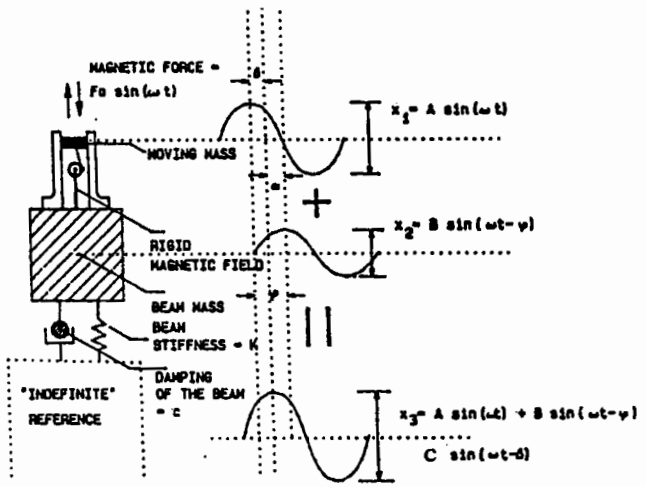

Figure 1. Absolute to relative amplitudes and phases relationship

The corresponding displacement response of the beam is

$$x_2 = B \sin(\omega t - \varphi) \qquad (2)$$

where : B = visible absolute amplitude coefficient of the excited mass

The accelerometers monitored absolute displacements, thus, the amplitude and phase angle relationship between the moving exciter mass and the excited beam were required to be investigated. The absolute displacement of the accelerometer positioned on the moving exciter mass is assumed as follows.

$$x_3 = x_1 + x_2 = C \sin(\omega t - \beta) \qquad (3)$$

where : C = visible absolute amplitude coefficient of the moving exciter mass.

The relationships amongst the amplitude coefficients, A, B, and C which will be referred to as amplitudes for the purpose of generality, and the phase angles φ and β are portrayed graphically in fig.1. Substituting trigonometric rules for x_1 and x_2 into equation (3) also yield

$$x_3 = A \sin \omega t + B \sin(\omega t - \varphi) \qquad (4)$$

Equating coefficients of equation (3) and (4) gives

$$A + B \cos \varphi = C \cos \beta \qquad (5)$$

$$B \sin \varphi = C \sin \beta \qquad (6)$$

To relate the phase angle in eq.(6) is divided by eq.(5) to give

$$\beta = \tan^{-1}\left[\frac{B \sin \varphi}{A + B \cos \varphi}\right]$$

Further, substituting eq.(6) into eq.(5) relates the amplitudes of the moving exciter mass to the amplitudes of the beam as

$$A = \frac{C}{\sin \varphi}[\sin(\varphi - \beta)] \qquad (8)$$

Introducing relative phase angle of the absolute displacement of the moving exciter mass to the absolute displacement of the excited beam, $\alpha = \varphi - \beta$ into equation (8), where the value of α is obtainable from steady state vibration experiments yields

$$A = \frac{C \sin \alpha}{\sin \varphi} \qquad (9)$$

Again, substituting $\alpha = \varphi - \beta$ into eq.(6) and rearranging the trigonometric identities gives

$$\varphi = \tan^{-1}\left[\frac{C \sin \alpha}{(C \cos \alpha - B)}\right] \qquad (10)$$

Equation (9) shows that the magnitudes of A and C depends on the ratio of ($\sin \alpha / \sin \varphi$). Since the value of α is always lower than the value of φ unless $\alpha = \varphi$ for all φ, and $\alpha = \varphi$ for $\varphi = 0, \pi, 2\pi$ .....etc..there will be a ratio of one within the value of $\varphi = 0$ to π. Thus, the amplitude, A (invisible) meets the amplitude, C (visible) within the range of $\varphi = 0$ to π. This can be obtained by substituting $A = C$ into equation (9) to give $\sin \varphi = \sin \alpha$. This exists only if :

a. $\varphi = 0, \pi, 2\pi, 3\pi$.....etc

b. $\varphi \geq \pi/2$ and $\varphi \leq \pi$ since $\varphi \geq \alpha$

In other word $\sin \varphi = \sin \alpha$ is possible only if $\varphi > \pi/2$ and $\alpha < \pi/2$. At this specific point of meeting $\cos \varphi = -\cos \alpha$. Including this identity into equation (10) gives

$$\frac{\sin \alpha}{-\cos \alpha} = \frac{C \sin \alpha}{C \cos \alpha - B} \quad ; \quad B = 2C \cos \alpha \qquad (11)$$

Effect of Reflected Force on Force of Excitation

The effect of the reflected force on the excitation force results in the jump phenomena appeared in the

mechanical exciter response and in a peculiar drop appeared in the magnetic exciter response (Priyosulistyo, 1988). To explain this, mathematically, a two degree of freedom system is considered. The moving exciter mass of the exciter is assumed to possess a lump mass, m and a stiffness from the magnetic field, k whilst the excited beam possesses a lump mass,M, stiffness,K and the damping coefficient,c. The moving exciter mass is subjected to a force $F_o \sin \omega t$ from the electro magnetic field. These relationships are graphically shown in fig.2.

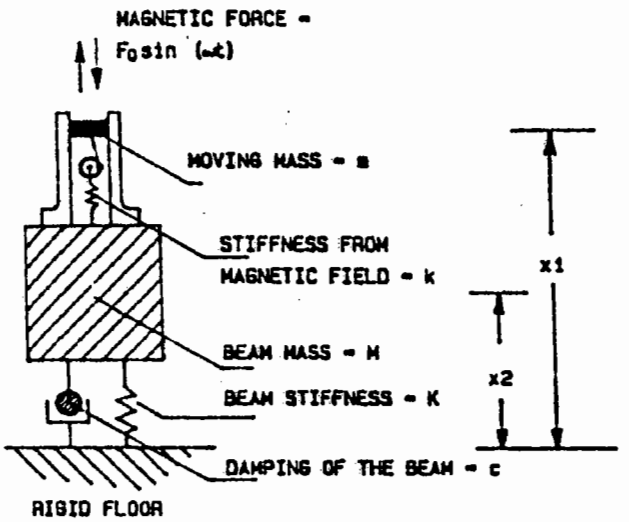

Figure 2. Mathematical model of beam investigated

The equation of motion of the moving exciter mass can be expressed as

$$F_o \sin \omega t = \mathrm{m}\, \ddot{x}_1 + k\, x_1 - k\, x_2 \qquad (12)$$

The particular solution to equation (12) may be represented as a combination of the force motion, A sin ωt and the reflected motion, B sin (ωt - φ) which has a phase with the excited beam. This combined motion can be expressed as

$$x_1 = A\sin\omega t + B\sin(\omega t - \varphi) = C\sin(\omega t - \beta) \qquad (13)$$

Amplitude coefficients A,B and C will be referred to as amplitudes for the purpose of generality. The equation of motion of the excited beam is

$$0 = M\, \ddot{x}_2 + K\, x_2 + k\, x_2 + c\, \dot{x}_2 - k\, x_1 \qquad (14)$$

The particular solution to eq.(14) is

$$x_2 = B\sin(\omega t - \varphi) \qquad (15)$$

Including the derivatives of equations (13) into equation (12) yield

$$F\sin\omega t = -m\omega^2 C\sin(\omega t-\beta) + kC\sin(\omega t-\beta) - kB\sin(\omega t \qquad (16)$$
$$= (k - m\omega^2)C\sin(\omega t-\beta) - kB\sin(\omega t-\varphi)$$

and also the derivatives of equation (15) into (14) yield

$$0 = -M\omega^2 B\sin(\omega t-\varphi) + KB\sin(\omega t-\varphi) + kB\sin(\omega t-\varphi) + c\omega B\cos(\omega t-\varphi) - kC\sin(\omega t-\beta) \qquad (17)$$
$$= (k + K - M\omega^2)B\sin(\omega t-\varphi) + c\omega B\cos(\omega t-\varphi) - kC\sin(\omega t-\beta)$$

Applying a trigonometric identity sin (ωt - β) = sin ωt cos β - cos ωt sin β into equation (16) and equating coefficients give

$$F = (k - m\omega^2)C\cos\beta - kB\cos\varphi \qquad (18)$$

$$0 = (k - m\omega^2)C\sin\beta - kB\sin\varphi \qquad (19)$$

Similar procedures are applied to equation (17) to give

$$0 = (k + K - M\omega^2)B\cos\varphi + c\omega B\sin\varphi - kC\cos\beta \qquad (20)$$
$$- kC\cos\beta$$

$$0 = (k + K - M\omega^2)B\sin\varphi - c\omega B\cos\varphi - kC\sin\beta \qquad (21)$$
$$- kC\sin\beta$$

Multiplying sin φ and cos φ into equation (20) and (21) respectively and summing those two equations gives

$$0 = c\omega B\,(\sin^2\varphi + \cos^2\varphi) - kC(\sin\varphi\cos\beta - \sin\beta\cos\varphi)$$
$$0 = c\omega B - kC\sin(\varphi - \beta)$$

Introducing relative phase angle $\alpha = \varphi - \beta$; $c = 2d^2 M p_2$; $k = m p_1$ gives

$$C = \frac{2d\,M\,p_2\,\omega B}{m\,p_1^2\sin\alpha}$$

Furthermore introducing $m_r = M/m$; $r_1 = \omega/p_1$; $p_r = p_2/p_1$ and $C_1 = 2d\ m_r p_r r_1$ gives

$$C = C_1 \quad B/\sin\alpha \qquad (22)$$

The amplitude, B of equation (22) can be obtained by substituting $C\cos\beta$ of equation (18) into (20).

$$0 = (k + K - M\omega^2)B\cos\varphi + c\omega B\sin\varphi - k\left[\frac{F + kB\cos\varphi}{(k - m\omega^2)}\right]$$

$$0 = (k - m\omega^2)(k + K - M\omega^2)B\cos\varphi + (k - m\omega^2)c\omega B\sin\varphi - kF - k^2 B\cos\varphi$$

Multiplying this later equation by $(1/k^2)$ gives

$$B = \frac{F/K}{\left[\left(1 + \frac{K - M\omega^2}{k}\right)\left(1 - \frac{m\omega^2}{k}\right)\cos\varphi + \frac{c\omega}{k}\left(1 - \frac{m\omega^2}{k}\right)\sin\varphi - \cos\varphi\right]}$$

Introducing $K = M p_2^2$, $k = m p_2^2$, $m_r = M/m$, $p_r = p_2/p_1$, $r_1 = \omega/p_1$ and $c = 2dMp_2^2$ give

$$B = \frac{F/k}{\{1+m_r(p_r^2-r_1^2)\}(1-r_1^2)\cos\varphi + 2dm_r p_1 r_1(1-r_1^2)\sin\varphi - \cos\varphi}$$

Substituting $C_1 = 2d\ m_r p_r r_1$; $C_2 = 1 + m_r (p_r^2 - r_1^2)$; $C_3 = (1 - r_1^2)$

$$B = \frac{F/k}{(C_2C_3 - 1)\cos\varphi + C_1C_3\sin\varphi} \qquad (23)$$

The phase angle, φ of equation (23) can be obtained by substituting C sin β of equation (19) into equation (21)

$$0 = (k + K - M\omega^2)B\sin\varphi - c\omega B\cos\varphi - k\left[\frac{kB\sin\varphi}{(k - m\omega^2)}\right]$$

$$0 = (k - m\omega^2)(k + K - M\omega^2)\sin\varphi - (k - m\omega^2)c\,\omega\cos\varphi - k^2\sin\varphi$$

$$\tan\varphi = \frac{c\omega(k - m\,\omega^2)}{(k - m\,\omega^2)(k + K - M\,\omega^2) - k^2}$$

Dividing the numerator and the denominator by k^2 give

$$\tan\varphi = \frac{c(\omega/k)(1 - m\omega^2/k)}{(1 - m\omega^2/k)(1 + (K/k) - M\omega^2/k) - 1}$$

$$= \frac{2dm_r p_r r_1(1 - r_1^2)}{(1 - r_1^2)(1 + m_r(p_2^2 - r_1^2)) - 1}$$

and from which φ can be expressed as

$$\varphi = \tan^{-1}\left[\frac{C_1C_3}{C_2C_3 - 1}\right] \qquad (24)$$

To evaluate the relative phase angle, α of equation (22) equation (18) and (19) are multiplied by cos φ and sin φ respectively.

$$F\cos\varphi = (k - m\omega^2)C\cos\beta\cos\varphi - kB\cos^2\varphi$$

$$0 = (k - m\omega^2)C\sin\beta\sin\varphi - kB\sin^2\varphi$$

By summing up the later equation and introducing the trigonometric rules those equations give

$$F\cos\varphi = (k - m\omega^2)C\cos(\varphi - \beta) - kB$$

Dividing by k the later equation gives

$$C = \frac{(F/k)\cos\varphi + B}{(1 - r_1^2)\cos\alpha} \qquad (25)$$

Equation (25) and (22) and introducing coefficients C_1, and C_3 give

$$\{(F/k)\cos\varphi + B\}/C_3\cos\alpha = C_1B/\sin\alpha$$

where :

$$\alpha = \tan^{-1}\left[\frac{C_1C_3B}{(F/k)\cos\varphi + B}\right] \qquad (26)$$

TEST PROCEDURES

Before applying the magnetic exciter the force characteristics were investigated. A force transducer (B & K type 8200) was screwed down on a thick steel plate, which was firmly anchored on the rigid concrete floor. Upon the force transducer the magnetic exciter was mounted. An accelerometer and a weight were also mounted on the moving exciter mass giving a total mass of 128.53 grams To avoid the additional effect of resonance of the body of the exciter on reading the data of the force transducer, only a low amplitude and a certain range of frequency of excitation were applied. This experiment calibrated force of excitation, which was deduced from the force-transducer and from the accelerator (multiplication of mass and relative acceleration).

A further study using the magnetic exciter was carried out (see fig. 3). Accelerometers measure absolute amplitudes. This implies that they are a means of measuring amplitudes and phases with respect to an 'indefinite' reference. The relative relationships of two accelerometers measuring absolute amplitudes (*C* and *B*) and phases (α, β, and φ), within the same'indefinite' time, reference and system, may be used to overcome this problem. The magnetic exciter (Derritron VP-2) was positioned on the beam at similar distance from the centre of the beams as the mechanical exciter. To increase the force of excitation 80 grams of mass and 29.93 grams of an accelerometer mass were added to the 18.6 grams of the built up moving mass. To measure relative amplitudes and phases of the moving exciter mass (inside the exciter, exciting the beam) to the beam under tests two accelerometers were employed. One accelerometer was mounted on the moving exciter mass and the other accelerometer was positioned on the beam close to the exciter. Both accelerometers measured absolute amplitudes and phases. The force

of excitation can be obtained by multiplying the total moving exciter mass, which was 128.53 grams, by its relative acceleration. A relative measuring device, the LVDT, was mounted to measure the relative displacement of the moving exciter mass to the body of the device. The frequency of excitation was controlled by turning the analog knob available on the integral amplifier. A low frequency digital indicator was employed to monitor the manually adjusted frequency increments. A decrease of voltage and an increase in ampere of the amplifier controlling the magnetic exciter about the beam resonance was monitored.

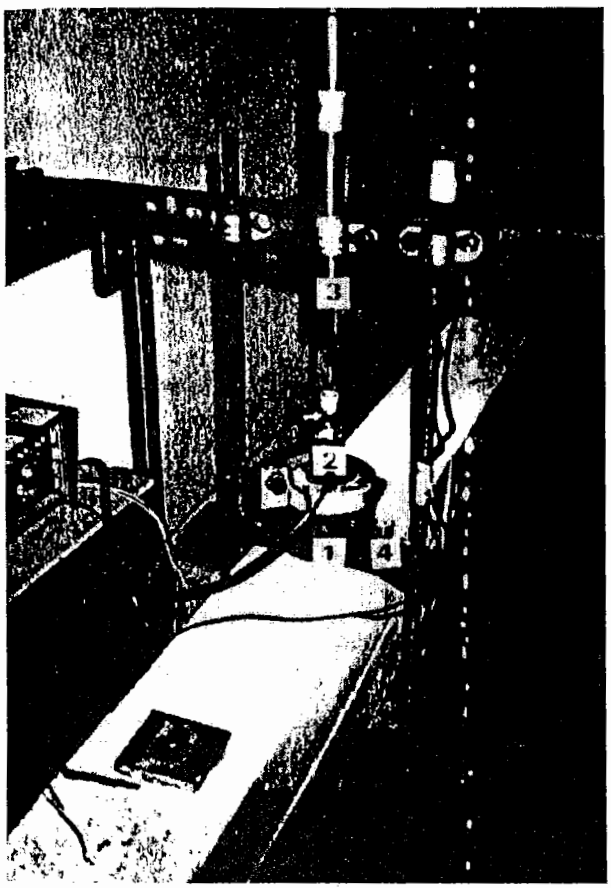

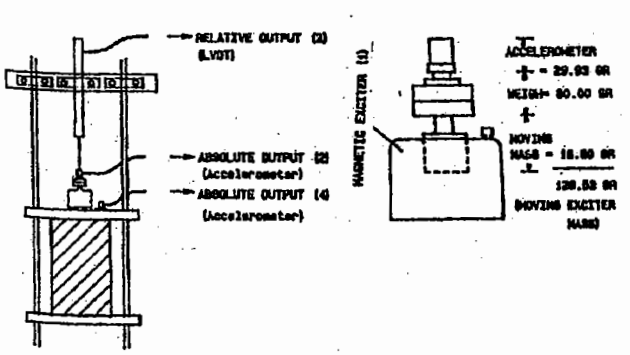

Figure 3. Experimental set up using magnetic exciter

Another experiment using the mechanical exciter was also set up (see fig.4). The moving half circle mass was arranged in two sets of angle (30 and 15 degree). Each set was applied in the experiment, with forward and reverse excitations. The increasing and decreasing frequencies of excitation were controlled using speed controller. The phase angles were determined by employing the amplitude response of accelerometer and the square signal from the optoswitch mounted on the exciter.

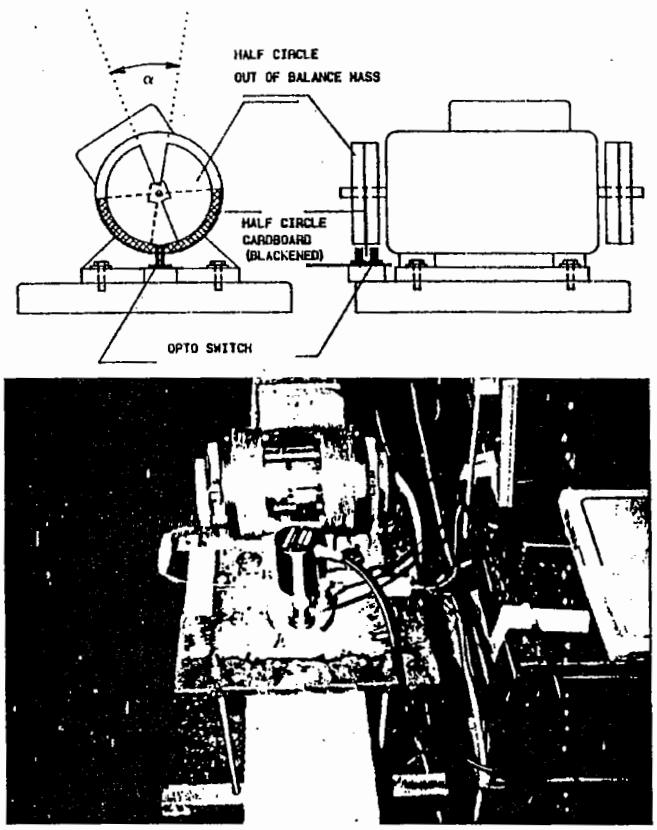

Figure 4. Experimental set up using mechanical exciter

RESULTS AND DISCUSSION

Calibration of Force of Excitation.

As the base of the magnetic exciter is fixed upon rigid structures with strong stiffness, therefore, equation 1 to 11 may be applied by taking B = 0, the force of excitation shown by the force transducer underneath the exciter is really equal to the multiplication of mass and acceleration (resulting from the mounted accelerometer), A = C. This also explains that both force transducer and accelerometer used in the experiment worked properly. Slight divergent results between 75 Hz and 275 Hz may be due to accident / mishandling during the experiment (see fig. 5).

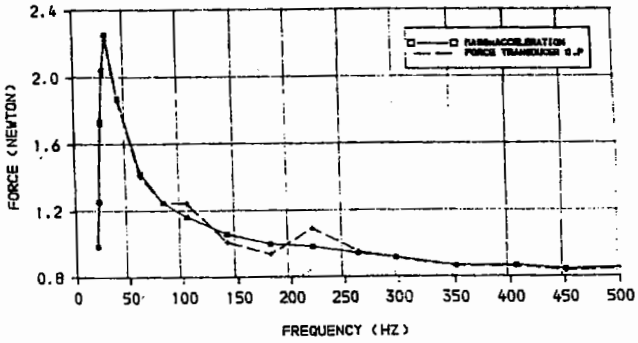

Figure 5. Calibration using force transducer and accelerometer

Experimental Jump Phenomenon.

Normalised frequency responses to the square of the frequency excitation in the hysteretic experiment (using the mechanical exciter) for different sets of force of excitation are shown in fig. 6. This experiment indicates that the unstable region causing the jump phenomenon depends on the force of excitation. The higher the force of excitation the larger the unstable region. This phenomenon is similar to non-linear hard spring behaviour demonstrated by White (1971) and Rades (1983) which was found from the membrane effect of a steel plate with simply supported hinges at its four edges and rubber or polyurethane pads for vibration isolation purposes. Polar diagrams as suggested by Rades (1982,1983), Tomlinson (1979,1980) and White (1971,1973) were also implemented to the test as shown in fig.7 indicates clearly the non-linear hard spring behaviour alike. The simple support system applied in the reinforced concrete beam experiment should not allow the non-linear hard-spring behaviour to occur. Thus, the unstable condition must have been due to something else.

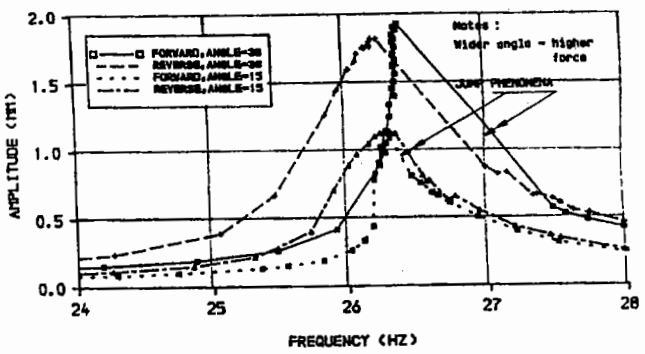

Figure 6. Response spectra of beam subject to mechanical exciter

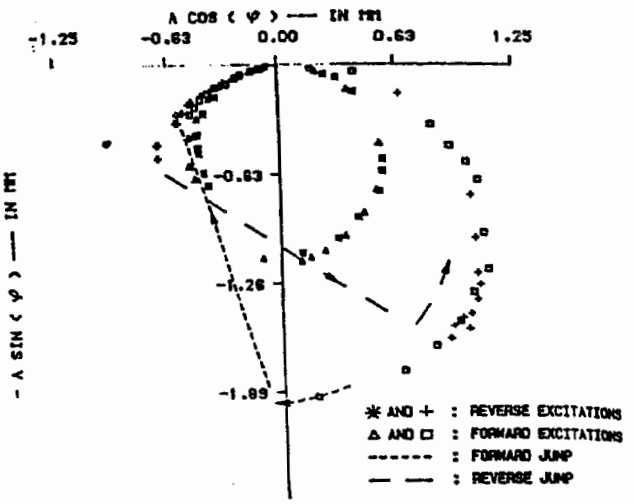

Figure 7. Related polar diagram of Figure-6.

The other experiment using the magnetic exciter of the same reinforced concrete beam as shown in fig.8 confirms that the jump phenomenon was not due to the non-linear hard-spring behaviour, but still possibly to occur. The response spectrum of the concrete beam subjected to a lower force of excitation (20-30 times lower) indicates that the jump phenomenon does not apparently exist. This confirms that the jump phenomenon seems to be force dependence. In contrast the amplitude of the moving exciter mass (both absolute and relative as shown by accelerometer on the moving exciter mass and the LVDT respectively) sharply decreases as the frequencies of excitation approaches the resonance.

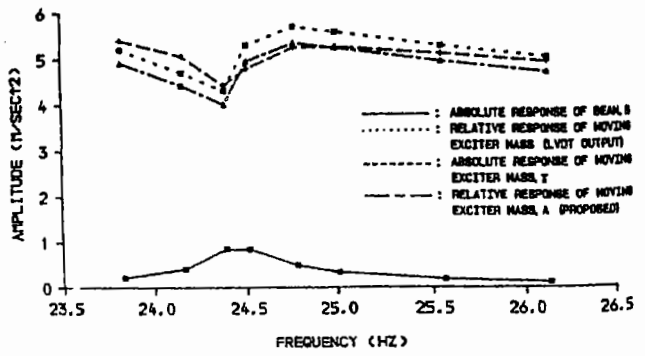

Figure 8. Response spectra of beam subject to magnetic exciter

This phenomenon also confirms the developed theory, assuming the presence of the absolute and relative amplitudes on the moving exciter mass, which are of interest when discussing normalised force of excitation. The reflected force of the excited beam is supposed to affect the amplitude of the moving exciter

mass. A further phenomenon is also indicated that the relative amplitudes of the LVDT are lower than the absolute amplitude of the accelerometer before approaching resonance and reversed after resonance. The relative phase difference measured from the LVDT to the excited beam and from the accelerometer to the excited beam as shown in fig.9 confirms the phenomenon mentioned above.

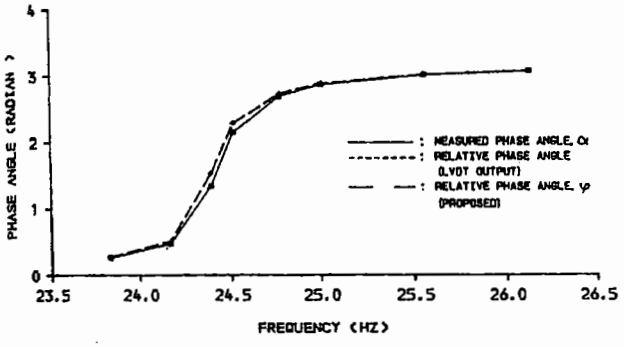

Figure 9. Phase relationship of Figure-8

Mathematical Approach.

Based on the calibration experiments, described in previous paragraph and established for those purposes, the relative amplitudes are determined using equation (9) and (10). The relative amplitudes resulting from equation (9) rely on the ratio of the sin α / sin φ. The calculated relative phase angles, φ are dependent on the measured amplitudes, *C* and *B* and the phase angle, α. These dependencies do not seem very critical since signal processing is carried out carefully. The measured relative displacements of the LVDT to the excited beam over the range of frequencies of the first mode shown in fig.8 are parallel to the calculated relative amplitudes,*A*. A slight difference is possibly due to different calibration factor. The absolute displacements before resonance overestimate the relative displacements. In contrast this phenomenon is reversed after resonance. The turning point represents a condition where the relative displacement, A is equal to the absolute displacement, C (B = 0, unstable). If the turning point is obtainable from the experiment then the relative phases can be determined from eq.(7) and e.q.(10) respectively. Further differences in the phase angles, as portrayed in fig. 9 for the same experiment, become significant about resonance. Those differences are obviously dependent on the amplitudes of the moving exciter mass and the excited beam.

Figure (10) indicates the sensitivity of the ratio of the relative to the absolute amplitudes, A/C over the phase of excitation, φ (0 to π). The higher the ratio of the absolute beam displacement to the relative amplitude of the moving exciter mass, r = (B/A) then the higher the ratio, A/C. This implies a means of obtaining the more significant differences between the absolute, C and the relative amplitude of the moving exciter mass,*A*. All curves in fig.10 pass a value of A/C = 1 but the higher phase of excitation, φ as the increase of the value of r.

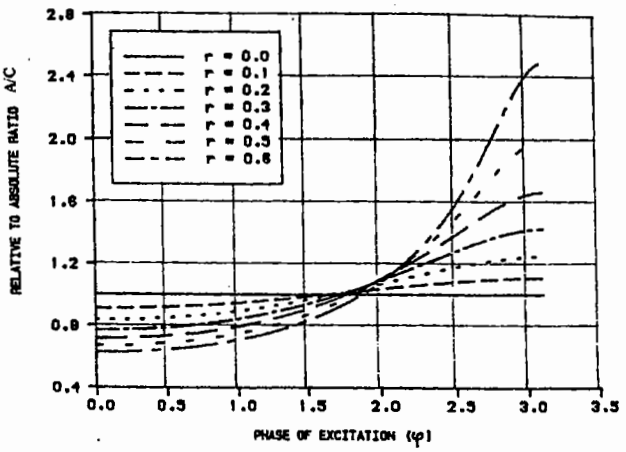

Figure 10. Sensitivity of amplitude ratio A/C and B/A over phase angle, φ

Applying equation (22) to (26) for m_r = 843.75 p_r = 14 and d = 10% with exponentially decreasing force results in the graph of fig.11 and fig.12. Fig.11 demonstrate the characteristics of the absolute amplitude response of the moving exciter mass,*C*. A significant drop occurs at about resonance as expected. The possibility of the jump phenomena as well as the sudden drop to occur increases proportionally with the force of excitation, but the damping ratio. The lower the damping ratio of the beam the greater the possibility of the sudden drop or the jump phenomena to occur. The reflected force opposes the excitation force in such a way that it reduces the amplitudes of the excitation. Response of the absolute amplitudes of the beam,*B* does not indicate any sudden drops or the jump phenomena (see fig.12). This graph is similar to the graph from the experimental data as shown in fig. 8. This simulation does not strongly approve the experimental results to great accuracy due to the simplifications used in the model but the method can approximately describe the behaviour of any exciter including the mechanical exciter used. The mechanical exciter has almost constant torque about the resonant frequencies. Due to the reflected force of the excited beam the out of balance mass movement was opposed. This was apparent as a decreasing speed/rotation of the out of balance mass. The reflected force reduces

the force of excitation at resonance but it is not possible to achieve dynamic equilibrium as the force of excitation increases proportionally to the square of the frequency of excitation. This creates an unstable condition. Thus, increasing the frequency, by increasing input power, will only pass by unstable region so producing the jump phenomenon as previously reported. The sensitivity of the reflected force depends on the mass ratio, m_r, frequency ratio,p_r, and damping ratio of the beam,d.

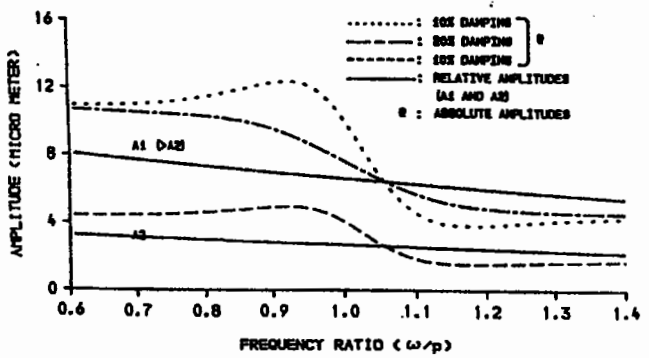

Figure 11. Effects of damping ratio on amplitudes at different force

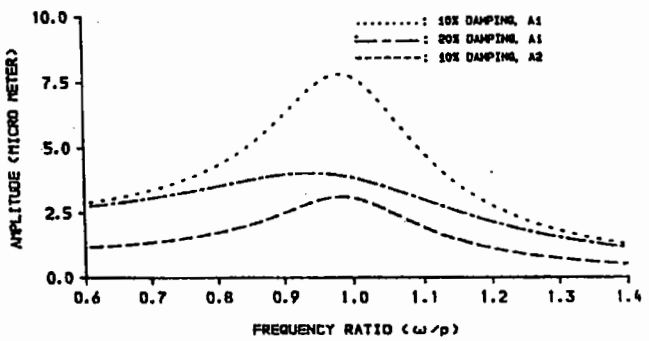

Figure 12. Response spectra of Figure-11

CONCLUSION

1. The experiments identified peculiar characteristics of two types of exciter, the magnetic and the mechanical exciters, over the resonance frequency.
2. Since the characteristics in question affect the response it is necessary to understand these characteristics. The phenomena are of interest since the maximum or resonance amplitude and the resonance frequency of the structure play an important role.
3. The response of the beam excited by the mechanical exciter displays a jump phenomenon and the response of the moving exciter mass of the magnetic exciter shows a sharp decrease in the amplitude about the resonance.
4. Mathematical models have been developed which reveal good understanding about the jump phenomena occurred in the experiments.

REFERENCES

Priyosulistyo,H., 1988, ***Vibration of Reinforced Concrete Beams,*** M.Sc. Thesis of the University of Strathclyde, U.K.

Rades,M., 1982, ***Parameter Identification of a Structure with Combined Coulomb and Hysteretic Damping***, Rev. Roum., Sci., Tech., mec, Appl., Tome 27, No.2, pp 299-308, Bucharest.

Rades,M., 1983, ***Identification of Dynamic Characteristics of a Simple System with Quadratic Damping***, Rev. Roum., Sci., Tech., mec, Appl., Tome 28, No.4, pp 439-446, Bucharest.

Rades,M., 1983, ***On the Effects of Non-linear Stiffness in Resonance Testing***, Rev. Roum., Sci., Tech., mec, Appl., Tome 28, No.6, pp 603-614, Bucharest.

Tomlinson,G.R., and Hibbert,J.H., 1979, ***Identification of the Dynamic Characteristics of Structures with Coulomb Friction***, Journal of Sound and Vibration, Vol.64, pp 233-242.

Tomlinson,G.R., 1980, ***An Analysis of Distortion Effects of Coulomb Damping on the Vector Plots of Lightly Damped Systems***, Journal of Sound and Vibration, 71(3), pp 443-451.

White, R.G., 1971, ***Effects of Non-linearity Due to Large Deflections in the Resonance Testing of Structures***, Journal of Sound and Vibrations, Vol.16, No.2, pp 255-267.

White, R.G., 1973, ***Effects of Non-linearity Due to Large Deflections in the Derivation of Frequency Response Data from the Impulse Response of Structures***, Journal of Sound and Vibrations, 29(3), pp 295-307.